

Reexamination of Slow Dynamics in Semidilute Solutions: From Correlated Concentration Fluctuation to Collective Diffusion

Guangcui Yuan,[†] Xiaohong Wang,[†] Charles C. Han,^{*,†} and Chi Wu^{*,‡}

State Key Laboratory of Polymer Physics & Chemistry, Joint Laboratory of Polymer Science & Materials, Institute of Chemistry, Chinese Academy of Sciences, Beijing 100080, People's Republic of China, and Department of Chemistry, The Chinese University of Hong Kong, Shatin, N.T., Hong Kong

Received January 10, 2006; Revised Manuscript Received March 26, 2006

ABSTRACT: Two different polymer systems, poly(*N*-isopropylacrylamide) (PNIPAM)/H₂O and poly(ethylene oxide)–poly(propylene oxide)–poly(ethylene oxide) (PEO–PPO–PEO)/H₂O, were examined by laser light scattering (LLS). In both cases, a single relaxation mode was observed in dilute solution which is related to the mutual diffusion of separated polymer chains. As the polymer concentration increases and enters the semidilute regime, one fast and one slow relaxation modes were observed. The fast mode corresponds to cooperative diffusion of chain segments inside each “blob”. Utilizing the thermal-sensitive properties of these two systems, we followed the disentanglement of transient network in the semidilute solutions through temperature-induced chain shrinkage, but without changing the overall concentrations. Meanwhile, we can follow the slow mode of the semidilute solution changes from long-range correlated concentration fluctuation of transient network to collective diffusion of aggregates or micelles. The present results clearly reveal that the slow modes in these two different systems have the same nature.

Introduction

Semidilute solutions of polymers have been the focus of attention for more than two decades. Because of the existence of overlapping and entanglement of polymer chains, new dynamical processes involving interchain interactions and disentanglement come into the problem. Many theoretical and experimental works have been invested to clarify the properties of these systems. Among these, dynamics and relaxation processes investigated by dynamic LLS are of particular interest. A number of dynamic LLS experiments on semidilute solutions have detected the deviation of the intensity–intensity time correlation function from a single-exponential decay, which is simultaneously with a fast and so-called slow mode.^{1–20} It is a widely held view that the fast mode is related to the cooperative diffusion of chain segments in each “blob”,²¹ while the slow mode has been assigned to a variety of origins, and the interpretation is far from a comprehensive resolution. For example, a general consensus in the angular, concentration, and chain length dependence and a clear understanding regarding the origins of the slow mode are still lacking.

For homopolymer in semidilute solutions, the origins of the slow mode have been mainly postulated to be related to reptation of a clustering of polymer chains through the entangled coils,^{1–4} or to the center-of-mass motion of the entire polymer chain in its surroundings,^{5–7} or to the viscoelastic properties of the network.^{14–17} As for block copolymer in a selective solvent, the chain dynamics in semidilute solutions is more complicated and system dependent, i.e., a good solvent for one block and a poor or nonsolvent for another block; segregation effects are responsible for a wide range of structures depending on the number of blocks, their degree of polymerization, their incompatibility, and the solvent quality.^{22,23} A common feature of these

systems is that multiple dynamic modes could be observed by dynamic LLS. The slow mode is tentatively attributed to cooperative rearrangements of microdomains,²⁴ or to cooperative diffusion of nodes,²⁵ or to viscoelastic relaxation of textures embedded in the solution,²⁶ or to “long-range density fluctuations” or “cluster” relaxation.^{27,28} The above interpretations about the origins of the slow mode are all speculative. In general, the slow modes observed in block copolymer systems are thought to be different in nature with that observed in homopolymer systems.²⁰

Actually, for polymers with high molecular weight, the overlap concentration (C^*) is low, and the semidilute regime extends to a low concentration (in terms of g L⁻¹),²⁹ where the segment density is so low that the extent of interpenetration or overlapping between polymer chains is rather limited. The precursor stage of a uniform transient network formation apparently extends over an unexpectedly broad concentration range where most of the reported experiments were carried out.³⁰ This precursor stage inevitably exists in all polymer/solvent systems, not depending on polymer chain structures. One possible explanation about the deviation of the intensity–intensity time correlation function measured in dynamic LLS from a single-exponential decay is that, in the experimental concentration range, the correlation of segments at different “blob” is not sufficiently “screened” by chain overlapping.²¹ In other words, the slow mode originates from the concentration fluctuation of segments belonging to different “blobs” in the solution which fluctuations take place dependently. The extent of correlation is directly related to the incorporation of various interactions, such as polymer–polymer, polymer–solvent, and solvent–solvent interaction, which can be attractive or repulsive.

In the present study, the system of PNIPAM/H₂O was selected because of its thermal-responsive properties which exhibits a lower critical solution temperature (LCST) around 32 °C,³² and the system of PEO–PPO–PEO/H₂O was selected because of the well-known fact that it can exhibit temperature-induced micellization phenomenon at a certain concentration range.³³ Although the homopolymer and the triblock copolymer have

* To whom correspondence should be addressed: Ph +86 010 82618089; Fax +86 010 62521519; e-mail c.c.han@iccas.ac.cn; e-mail chiwu@cuhk.edu.hk.

[†] The Institute of Chemistry, CAS.

[‡] The Chinese University of Hong Kong.

great difference in chain structures, the advantage of using these two systems is that we are able to utilize the temperature dependence of the solvent–polymer interaction to investigate effects of the shrinkage of polymer chains with increasing temperature, and consequently disentanglement of transient network, on all the corresponding (slow and fast) modes in the semidilute regime. In this article, through following the slow mode in semidilute solutions changes from long-range correlated concentration fluctuation to collective diffusion, we wish to show that the slow modes in these two systems before aggregation (for PNIPAM/H₂O system) or micellization (for PEO–PPO–PEO/H₂O) have the same nature, reflecting long-range correlated concentration fluctuation, like the internal motion of a transient network.

Experimental Section

Sample Preparation. The free radical polymerization of PNIPAM was adopted from a procedure reported by Zhou and co-workers.³⁴ The monomer *N*-isopropylacrylamide (ACROS) was recrystallized three times from a benzene/*n*-hexane mixture, and the initiator azobis(isobutyronitrile) was recrystallized twice from methanol. The PNIPAM was filtered and fractionated in acetone/*n*-hexane mixture at room temperature. One of the fractionated samples was used in the present study with $M_n = 1.99 \times 10^5$ g mol⁻¹ and $M_w/M_n = 1.1$, measured by gel permeation chromatography (Waters) at 20 °C with tetrahydrofuran as eluant. Solutions were cleared with the use of 0.45 μm Millipore filters individually into dust-free light scattering cells at about 20 °C. The PEO–PPO–PEO triblock copolymer was purchased from Aldrich Chemical Co. The total molecular weight is 14 600, and the total content of PEO is 82.5 wt %, namely, about 137 + 137 units of ethylene oxide and 44 units of propylene oxide. Solutions were prepared individually at 4 °C followed by filtration through 0.22 μm Millipore filters directly into a dust-free light scattering cell. The cells were sealed to prevent any leakage of solvent. All solutions were prepared with Milli-Q water. Solutions were in each case allowed to stand after filtering for 1 week prior to measurement. The samples were allowed to equilibrate for ca. 3 h at each measurement temperature before the LLS experiments were commenced, unless indicated otherwise.

Laser Light Scattering. A commercial LLS spectrometer (ALV/DLS/SLS-5022F) equipped with a multi- τ digital time correlator (ALV5000) and a cylindrical 22 mW UNIPHASE He–Ne laser ($\lambda_0 = 632.8$ nm) was used. The spectrometer has a high coherence factor of $\beta \sim 0.95$ because of a novel single-mode fiber optical coupled with an efficient avalanche photodiode. The LLS cell is held in a thermostat index matching vat filled with purified and dust-free toluene, with the temperature controlled to within ± 0.02 °C. The details of the LLS instrumentation and theory can be found elsewhere.^{35,36} In dynamic LLS, the intensity–intensity time correlation function $G^{(2)}(t, q)$ in the self-beating mode was measured, where t is the decay time and q is scattering vector ($q = (4\pi n/\lambda_0) \sin(\theta/2)$). $G^{(2)}(t, q)$ can be related to the normalized first-order electric field time correlation function $|g^{(1)}(t, q)|$ via the Siegert relation as³⁶

$$G^{(2)}(t, q) = A[1 + \beta |g^{(1)}(t, q)|^2] \quad (1)$$

where $A (\equiv \langle I(0) \rangle^2)$ is the measured baseline. For the broadly distributed relaxation spectrum, $|g^{(1)}(t, q)|$ is related to a characteristic relaxation time distribution $G(\tau)$ as

$$|g^{(1)}(t, q)| \equiv \langle E(0, q) E^*(t, q) \rangle / \langle E(0, q) E^*(0, q) \rangle = \int_0^\infty G(\tau) e^{-t/\tau} d\tau \quad (2)$$

$G(\tau)$ can be calculated from the Laplace inversion of the measured $G^{(2)}(t, q)$ on the basis of eqs 1 and 2. In this study, the CONTIN program supplied with the correlator was used.³⁷

Results and Discussion

The radius of gyration of PNIPAM sample at 25.0 °C determined by static light scattering from a Zimm plot³⁸ is R_g

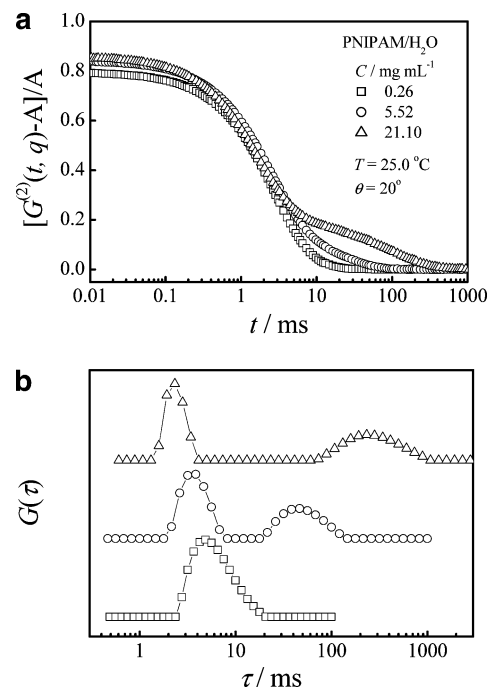


Figure 1. (a) Concentration dependence of intensity–intensity time correlation function $[G^{(2)}(t, q) - A]/A$ and (b) their corresponding characteristic relaxation time distribution function $G(\tau)$ of PNIPAM/H₂O in both dilute and semidilute regimes.

$= 35.1$ nm. The overlap concentration of the PNIPAM sample estimated from $3M_w/(4\pi N_A R_g^3) < C^* < M_w/(N_A (\sqrt{2} R_g)^3)$ to be in the range 1.9–2.8 mg mL⁻¹. The average hydrodynamic radius of PEO–PPO–PEO unimers is 3.7 nm measured by dynamic LLS. According to Burchard,³⁹ we estimated R_g of the unimers to be about 6.7 nm. Therefore, the overlap concentration of the PEO–PPO–PEO sample estimated to be in the range 19.0–28.0 mg mL⁻¹. It is important to note that C^* is not a critical concentration, and there is no established consensus about the definition of the overlap concentration.²¹

For PNIPAM in semidilute aqueous solutions, Hirotsu and co-workers⁴⁰ found that the correlation function measured by dynamic LLS could be fitted to single-exponential quite well through the whole temperature range investigated (25–40 °C). They claimed that the translation motion of polymer molecules is profoundly inhibited due to the relative immobility of densely packed coils and the intermolecular entanglement effect; the correlation function represents the relaxation of the internal or pseudo-gel motion. Bianco-Peled and co-workers⁴¹ used small-angle neutron scattering to measure the effect of salts on the conformation and microstructure of PNIPAM in aqueous solution. At temperatures well below the phase-transition temperature, the semidilute solutions exhibit the behavior predicted by the model of dynamic concentration fluctuations characterized by a single correlation length. However, as will be shown below, our present study found that the single relaxation mode measured from dilute PNIPAM aqueous solution by dynamic LLS turns into one fast and one slow relaxation modes when the concentration enters into the semidilute regime. Figure 1a shows typical plots of the intensity–intensity correlation function for the PNIPAM/H₂O system in both the dilute and semidilute regimes, and Figure 1b shows the corresponding plots of characteristic relaxation time distribution function analyzed by the CONTIN method. When $C < C^*$, a single relaxation mode is observed, which is related to the mutual diffusion of individual polymer chains. As the concentration increases and enters the semidilute regime,

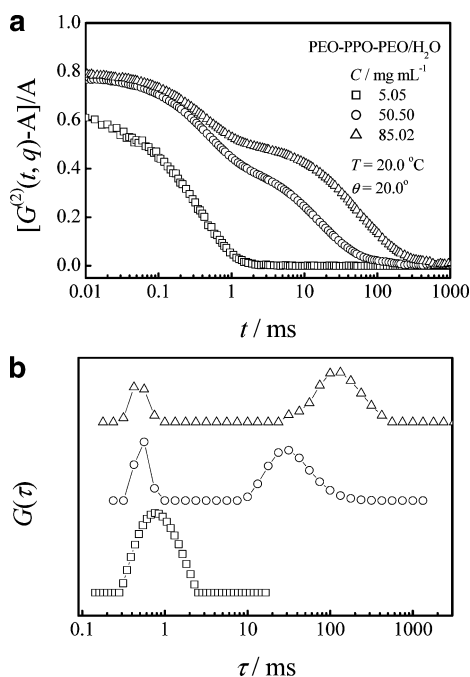


Figure 2. (a) Concentration dependence of intensity-intensity time correlation function $[G^{(2)}(t, q) - A]/A$ and (b) their corresponding characteristic relaxation time distribution function $G(\tau)$ of PEO-PPO-PEO/H₂O in both dilute and semidilute regimes.

the chains begin to overlap and entangle, and new dynamical processes involving interchain interaction and disentanglement begin to occur besides the fast relaxation mode. The slow mode becomes more and more evident, and its characteristic relaxation time shifts toward slow direction with increasing concentrations.

Figure 2a shows typical plots of intensity-intensity correlation function for the PEO-PPO-PEO/H₂O system in both the dilute and semidilute regimes, and Figure 2b shows the corresponding plots of characteristic relaxation time distribution function analyzed by the CONTIN method. The apparent coherence is lower for dilute solution in Figure 2a due to its weak scattering intensity. The same tendency with that in the PNIPAM/H₂O system can be seen as increasing concentrations. Here, $T = 20.0$ °C is below the critical micellization temperature (cmt) of all the mentioned concentrations according to Hatton et al.⁴² The slow mode is also observed at lower temperatures (e.g., 10.0 °C) but not shown here. The slow mode is 2 orders of magnitude slower than the fast mode, for PNIPAM/H₂O at the concentration which is about twice C^* , but the slow mode is 3 orders of magnitude slower than the fast mode, for PEO-PPO-PEO/H₂O at the concentration which is about twice C^* . The difference in magnitude between the slow mode and the fast mode could be related to the solvation conditions and possible interactions.⁴

The average characteristic relaxation rate ($\langle\Gamma\rangle = 1/\langle\tau\rangle$) is obtained from the moments of the peaks in the relaxation time distribution or, if the peaks are overlapping with each other, from the peak positions. In Figure 3 (for the PNIPAM/H₂O system) and Figure 4 (for the PEO-PPO-PEO/H₂O system), plots of the average characteristic relaxation rate of fast modes $\langle\Gamma_f\rangle$ ($= 1/\langle\tau_f\rangle$) vs q^2 are all straight lines through the origin. It clearly reveals the diffusive character of these relaxations because $\langle\Gamma\rangle$ can be related to q^2 by $\langle\Gamma\rangle = \langle D \rangle q^2$ for the diffusive motion.

Dynamic LLS measures the mutual diffusion coefficient ($\langle D_m \rangle$) in dilute solution, which increases (or decreases) slightly with increasing polymer concentrations in good solvent (or in

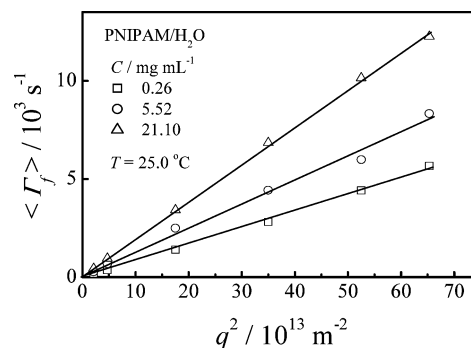


Figure 3. Scattering vector (q) and concentration dependence of average characteristic relaxation rate ($\langle\Gamma_f\rangle$) of fast relaxation mode for the PNIPAM/H₂O system.

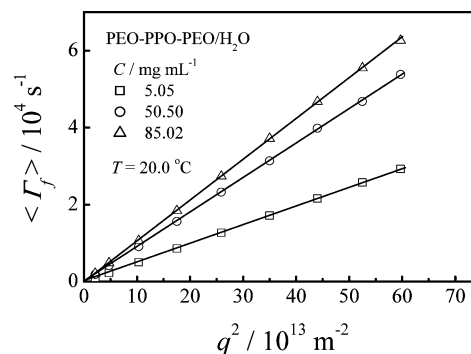


Figure 4. Scattering vector (q) and concentration dependence of average characteristic relaxation rate ($\langle\Gamma_f\rangle$) of fast relaxation mode for the PEO-PPO-PEO/H₂O system.

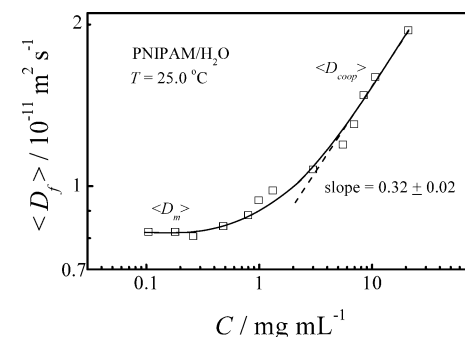


Figure 5. Concentration dependence of mutual diffusion coefficient ($\langle D_m \rangle$) (when $C < C^*$) and cooperative diffusion coefficient ($\langle D_{coop} \rangle$) (when $C > C^*$) for the PNIPAM/H₂O system.

Θ solvent).⁴³ As the solution enters into the semidilute regime, the diffusion coefficient is called cooperative diffusion coefficient ($\langle D_{coop} \rangle$), for it represents cooperative motion of chain segments within each “blob”. $\langle D_{coop} \rangle$ increases in a power law with increasing concentrations as predicted by the scaling theory for linear homopolymer chains in the semidilute regime: $\langle D_{coop} \rangle \sim C^{3/4}$ in good solvent conditions and $\langle D_{coop} \rangle \sim C$ in Θ solvent conditions.^{31,43} The concentration dependence of $\langle D_m \rangle$ and $\langle D_{coop} \rangle$ is shown in Figure 5 (for the PNIPAM/H₂O system) and Figure 6 (for the PEO-PPO-PEO/H₂O system) in a double-logarithmic scale. The fast modes of these two different systems show similar behavior. With an increasing concentration, $\langle D_m \rangle$ changes linearly and slightly, followed by a sharp upturn to a crossover to $\langle D_{coop} \rangle$ in the semidilute regime. Dynamic LLS studies on PEO-PPO-PEO copolymers in aqueous solutions over a wide range of concentration and temperature up to the cloud point were amply reported previously by many groups.^{44–47} However, the main emphasis of these efforts was placed on the phenomena of anomalous

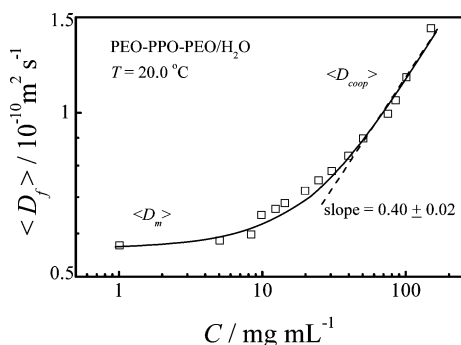


Figure 6. Concentration dependence of mutual diffusion coefficient ($\langle D_m \rangle$) (when $C < C^*$) and cooperative diffusion coefficient ($\langle D_{\text{coop}} \rangle$) (when $C > C^*$) for the PEO-PPO-PEO/H₂O system.

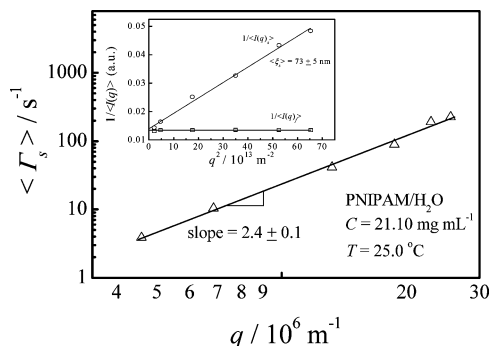


Figure 7. Scattering vector (q) dependence of average characteristic relaxation rate ($\langle \Gamma_s \rangle$) of slow relaxation mode for a semidilute aqueous solution of PNIPAM. The inset shows the scattering vector (q) dependence of reciprocal time-averaged scattering intensity ($\langle I(q) \rangle$) of the fast and slow modes.

association and mechanism of micelle/gel transition, and the concentration effects on chains overlaps or entanglement are neglected. Therefore, even though one fast and one slow modes at certain temperature range in moderately (semidilute) solutions have been observed before, their explanation has been that the fast and slow modes are respectively corresponding to the motions of the unimers and large aggregates. Taking our present results into account, we consider that the fast mode for PEO-PPO-PEO/H₂O in the semidilute regime is related to cooperative diffusion of chain segments in a “blob”, like that for PNIPAM/H₂O in the semidilute regime, but not diffusive motion of a total unimer as interpreted by many previously reports.^{46,47} $\langle D_{\text{coop}} \rangle$ can be related to the average dynamic correlation length $\langle \xi_D \rangle$ (equal to the “blob” size) by $\langle \xi_D \rangle = k_B T / (6\pi\eta_0 \langle D_{\text{coop}} \rangle)$. It is understandable that $\langle \xi_D \rangle$ decreases with an increasing polymer concentrations where the number of entanglement points increases. $\langle D_{\text{coop}} \rangle$ increases in a power law with an exponent about 0.32 (Figure 5) and 0.40 (Figure 6), which are much smaller than that predicted by the scaling theory. The interpretation to the obvious deviation of the exponent is that the power law works in the range where it should fail according to the scaling theory.^{8,14,31}

As for the slow mode, Figure 7 (for the PNIPAM/H₂O system) and Figure 8 (for the PEO-PPO-PEO/H₂O system) show that $\langle \Gamma_s \rangle (= 1/\langle \tau_s \rangle)$ can be scaled to q as $\langle \tau_s \rangle \sim q^{\alpha_s}$ with $2 < \alpha_s < 3$. It has been shown that the value of α_s is related to the ratio of the observation length scale ($1/q$) in LLS to the static correlation length ($\langle \xi_s \rangle$). The exponent α_s approaches 2 when $\langle \xi_s \rangle \ll 1/q$; α_s approaches 3 when $\langle \xi_s \rangle \gg 1/q$ and $a \ll 1/q$ (where a is the statistical segment length) and $2 < \alpha_s < 3$ when $\langle \xi_s \rangle \sim 1/q$, in the transition region.^{31,48–50} Here, the value of α_s indicated that the length scale of the slow relaxation is

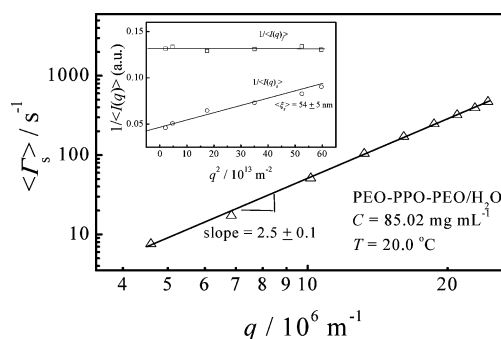


Figure 8. Scattering vector (q) and concentration dependence of average characteristic relaxation rate ($\langle \Gamma_s \rangle$) of slow relaxation mode for a semidilute aqueous solution of PEO-PPO-PEO/H₂O. The inset shows the scattering vector (q) dependence of reciprocal time-averaged scattering intensity ($\langle I(q) \rangle$) of the fast and slow modes.

comparable with the observation length ($1/q$) in LLS. If we assume that the two relaxation modes are “monodisperse”, which is not exactly correct in reality, an approximation can be obtained: the time-averaged scattering light intensity of solution $\langle I(q) \rangle$ comes from uncorrelated chain segments or “blobs” $\langle I(q)_f \rangle$ and correlated chain segments or “cluster” $\langle I(q)_s \rangle$, where the solvent contribution has been neglected, namely, with $\langle I(q) \rangle = \langle I(q)_f \rangle + \langle I(q)_s \rangle$ and $\langle I(q)_f \rangle = \langle I(q) \rangle A_f$, $\langle I(q)_s \rangle = \langle I(q) \rangle A_s$, and $A_f + A_s = 1$, where A_f and A_s are the intensity weighting of the fast and slow modes, respectively. It has been known that the static correlated length ξ can be related to the scattering intensity $I(q)$ and the scattering vector q by the Ornstein–Zernike equation:^{51,52}

$$I(q) = \frac{I(q \rightarrow 0)}{1 + q^2 \xi^2} \quad (3)$$

The slope-to-intercept ratio leads to the static correlated length from the plot of $1/I(q)$ vs q^2 . The insets in Figure 7 and Figure 8 show that the $\langle I(q)_f \rangle$ does not show an angular dependence, indicating that the “blob” size is much less than $1/q$, and the static correlation lengths of the slow mode are comparable with $1/q$ (for example, $\theta = 90^\circ$, $1/q = 53$ nm), which is consistent with the dynamic light scattering results. That is, the slow mode observed in the semidilute region is related to long-range correlated concentration fluctuation, like internal motion of a transient network. The extent of correlation is enhanced in the high extent of interpenetration of polymer chains, where the disentanglement effect is weakened. As proved above, for PEO-PPO-PEO/H₂O in the semidilute regime, the fast mode reflects the cooperative diffusion of chain segments and the slow mode should be related to chains overlapping or entanglement, but not with aggregates of unknown structures induced by chemical heterogeneity.^{46,47} The effect of chemical heterogeneity, which will result in anomalous association, is nonsignificant in this triblock copolymer with a high PEO content.

For PNIPAM in aqueous medium, temperature affects the balance between hydrophilicity and hydrophobicity and thus the polymer conformation. When the temperature is above the LCST of a certain semidilute solution, the polymer chains tend to undergo phase separation (or aggregation).³² Figure 9 shows the temperature dependence of characteristic relaxation time distribution function obtained from a semidilute solution. The data on the x -axis is shifted by (T/η_0) so that the peak positions at different temperatures can be directly compared, where η_0 is the solvent viscosity at the absolute temperature. It is clear that the fast mode shifts to the slower direction while the slow mode becomes faster with increasing temperatures when $T < 30.0$

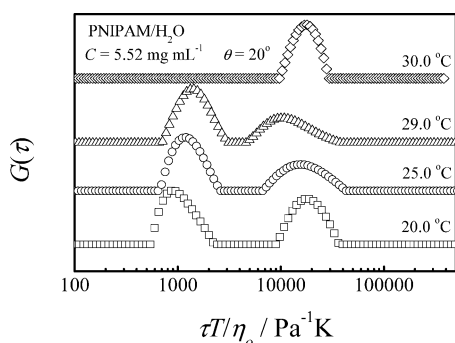


Figure 9. Temperature dependence of characteristic relaxation time distribution function $G(\tau)$ for a semidilute aqueous solution of PNIPAM.

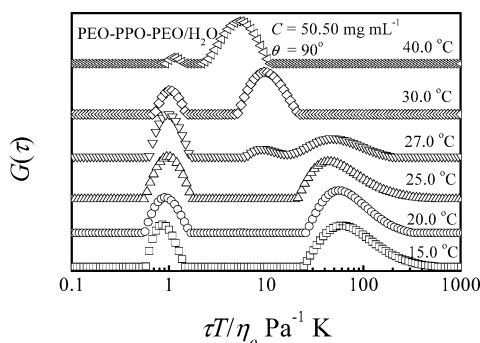


Figure 10. Temperature dependence of characteristic relaxation time distribution function $G(\tau)$ for a semidilute aqueous solution of PEO-PPO-PEO.

°C. The effects are just contrary to that of increasing concentrations. The solvent quality tends to be poor with increasing temperature, which will result in shrinkage of polymer chains. For semidilute solutions of polymer chains with a finite length, the shrinkage of polymer chains will result in fewer entanglement points and, consequently, a loose network with more defects or larger structural fluctuation. However, at $T = 30.0$ °C, phase separation happens. It should be noted that measurements at this temperature do not deal with a system at thermodynamic equilibrium but are controlled by kinetic processes. After isothermal for 32 h at this temperature, the characteristic relaxation time distribution function turns out to be single narrow mode, which is q^2 -dependent and related to collective diffusion of aggregates.

For nonionic polymeric surfactants PEO-PPO-PEO triblock copolymer in aqueous solutions, the dehydration gradually becomes significant with increasing temperature and consequently results in a decrease of the size of copolymer chains. When the temperature is above the cmc of a certain concentration, micelles will form. Figure 10 shows the temperature dependence of characteristic relaxation time distribution function obtained from a semidilute solution. Below 25.0 °C, the same tendency of fast mode and the slow mode changing with temperature was observed, compared with that in the PNIPAM/H₂O system. With increasing temperature, it is clear that an intermediate mode appears accompanied by the disappearance of the slow mode. The intermediate mode is evident at high temperature, and its relaxation rate is q^2 -dependent; therefore, it can be interpreted as collective diffusion of micelles. In summary, the nature of the fast mode and the slow mode in these two different systems appear to be the same. The difference is that, after the network break, aggregates are formed in the PNIPAM/H₂O system, but micelles are formed in the PEO-PPO-PEO/H₂O system.

Conclusion

The main point presented is that the origins of slow modes observed in semidilute solutions of homopolymer system (PNIPAM/H₂O) and of triblock copolymer system (PEO-PPO-PEO/H₂O) are the same. In both systems, concentration and temperature effects on the chain dynamics were studied by dynamic LLS. Although these two kinds of polymer have great difference in their chain structures, they show similar behaviors. The single fast relaxation mode in dilute solution, corresponding to the mutual diffusion of fully dispersed polymer chains, remains when the solution enters the semidilute regime. However, as the concentration increases, this fast mode becomes faster, together with the appearance of an additional slow mode caused by overlapping or entanglement of polymer chains. The characteristic relaxation rate $\langle\Gamma_f\rangle$ of the fast mode is q^2 -dependent, indicating its diffusive nature. Such a fast relaxation mode is related to the cooperative diffusion of the chain segments of each "blob" in semidilute solutions. The characteristic relaxation rate $\langle\Gamma_s\rangle$ of the slow mode can be scaled to q as $\langle\Gamma_s\rangle \sim q^{\alpha_s}$, with $2 < \alpha_s < 3$. This can be interpreted as the long-range concentration fluctuations of the correlated polymer chains in the transient network. The special thermal-sensitive properties of these two systems enable us to follow the temperature-induced shrinkage of polymer chains and, consequently, disentanglement of transient network in semidilute solutions formed by overlapped or entangled polymer chains, without changing the overall concentration. The fast mode shifts to slower direction, the slow mode shifts to faster direction with increasing temperature, and finally the slow mode corresponding to long-range concentration turns into a collective diffusion mode. The difference between these two systems is that aggregates are formed in the PNIPAM/H₂O system but micelles are formed in the PEO-PPO-PEO/H₂O system, while the transient networks are completely broken.

Acknowledgment. This work has been supported by the Chinese Academy of Sciences (Grant KJCX2-SW-H07), the Ministry of Science and Technology of China (Grant 2003-CB615600), and the Chinese National Science Foundation (Project 20490220).

References and Notes

- (1) Nose, T.; Chu, B. *Macromolecules* **1979**, *12*, 590, 599.
- (2) Chu, B.; Nose, T. *Macromolecules* **1980**, *13*, 122.
- (3) Lin, Y.-H.; Chu, B. *Macromolecules* **1981**, *14*, 385, 392.
- (4) Chu, B. *Polym. J.* **1985**, *17*, 225.
- (5) Amis, E. J.; Han, C. C. *Polymer* **1982**, *23*, 1403.
- (6) Amis, E. J.; Han, C. C.; Matsushita, Y. *Polymer* **1984**, *25*, 650.
- (7) Nishio, I.; Wada, A. *Polym. J.* **1980**, *12*, 145.
- (8) Schaefer, D. W.; Lin, J. S. *Macromolecules* **1983**, *16*, 1015.
- (9) Eisele, M.; Burchard, W. *Macromolecules* **1984**, *17*, 1636.
- (10) Hwang, D.-H.; Cohen, C. *Macromolecules* **1984**, *17*, 1679, 2890.
- (11) Brown, W.; Johnsen, R. M.; Stilbs, P. *Polym. Bull. (Berlin)* **1983**, *9*, 305.
- (12) Brown, W.; Johnsen, R. M. *Macromolecules* **1985**, *18*, 379.
- (13) Brown, W.; Štěpánek, P. *Macromolecules* **1988**, *21*, 1791.
- (14) Brown, W.; Nicolai, T. *Colloid Polym. Sci.* **1990**, *268*, 977.
- (15) Brown, W.; Štěpánek, P. *Macromolecules* **1992**, *25*, 4359.
- (16) Brown, W.; Štěpánek, P. *Macromolecules* **1993**, *26*, 6884.
- (17) Faraone, A.; Magazù, S.; Maisano, G.; Ponterio, R.; Villari, V. *Macromolecules* **1999**, *32*, 1128.
- (18) Sun, T.; King, H. E., Jr. *Macromolecules* **1996**, *29*, 3175.
- (19) Ngai, T.; Wu, C. *Macromolecules* **2003**, *36*, 848.
- (20) Ngai, T.; Wu, C.; Chen, Y. *Macromolecules* **2004**, *37*, 987.
- (21) Fujita, H. *Polymer Solutions*; Elsevier: Amsterdam, 1990.
- (22) Tuzar, Z.; Kratochvil, P. *Surf. Colloid Sci.* **1992**, *15*, 1.
- (23) Halperin, A.; Tirrell, M.; Lodge, T. P. *Adv. Polym. Sci.* **1992**, *100*, 31.
- (24) Balsara, N. P.; Štěpánek, P.; Lodge, T. P.; Tirrell, M. *Macromolecules* **1991**, *24*, 6227.

- (25) Raspaud, E.; Lairez, D.; Adam, M.; Carton, J.-P. *Macromolecules* **1996**, *29*, 1269.
- (26) Klucker, R.; Munch, J. P.; Schosseler, F. *Macromolecules* **1997**, *30*, 3839.
- (27) Jian, T.; Anastasiadis, S. H.; Semenov, A. N.; Fytas, G.; Adachi, K.; Kotaka, T. *Macromolecules* **1994**, *27*, 4762.
- (28) Nyström, B.; Walderhaug, H.; Hansen, F. K. *J. Phys. Chem.* **1993**, *97*, 7743.
- (29) Doi, M. *Introduction to Polymer Physics*; Oxford University Press: Clarendon, 1996.
- (30) Koberstein, J. T.; Picot, C.; Benoit, H. *Polymer* **1985**, *26*, 673.
- (31) Schaefer, D. W.; Han, C. C. In *Dynamic Light Scattering*; Pecora, R., Ed.; Plenum: New York, 1985.
- (32) Schild, H. G. *Prog. Polym. Sci.* **1992**, *17*, 163.
- (33) Chu, B. *Langmuir* **1995**, *11*, 414.
- (34) Zhou, S. Q.; Fan, S. Y.; Au-yeung, S. T.; Wu, C. *Polymer* **1995**, *36*, 1341.
- (35) Chu, B. *Laser Light Scattering*; Academic Press: New York, 1974.
- (36) Berne, B. J.; Pecora, R. *Dynamic Light Scattering*; Plenum Press: New York, 1976.
- (37) Provencher, S. W.; Hendrix, J.; Maeyer, L. D.; Paulussen, N. *J. Chem. Phys.* **1978**, *69*, 4273.
- (38) Zimm, B. H. *J. Chem. Phys.* **1948**, *16*, 1099.
- (39) Burchard, W. In *Light Scattering: Principles and Development*; Brown, W., Ed.; Clarendon Press: Oxford, 1996.
- (40) Yamamoto, I.; Iwasaki, K.; Hirotsu, S. *J. Phys. Soc. Jpn.* **1989**, *51*, 210.
- (41) Krasovitski, E.; Cohen, Y.; Bianco-Peled, H. *J. Polym. Sci., Part B: Polym. Phys.* **2004**, *42*, 3713.
- (42) Alexandridis, P.; Holzwarth, J. F.; Hatton, T. A. *Macromolecules* **1994**, *27*, 2414.
- (43) Teraoka, I. *Polymer Solutions*; Wiley: New York, 2002.
- (44) Nyström, B.; Kjønksen, A. L. *Langmuir* **1997**, *13*, 4520.
- (45) Zhou, Z. K.; Chu, B. *Macromolecules* **1988**, *21*, 2548.
- (46) Brown, W.; Schillén, K.; Almgren, M.; Hvidt, S.; Bahadur, P. *J. Phys. Chem.* **1991**, *95*, 1850.
- (47) Brown, W.; Schillén, K.; Hvidt, S. *J. Phys. Chem.* **1992**, *96*, 6038.
- (48) Dubois-Violette, E.; de Gennes, P. G. *Physics* **1967**, *3*, 181.
- (49) Akcasu, A. Z.; Benmouna, M.; Han, C. C. *Polymer* **1980**, *21*, 866.
- (50) Lodge, T. P.; Han, C. C.; Akcasu, A. Z. *Macromolecules* **1983**, *16*, 1180.
- (51) Bueche, F. J. *Colloid Interface Sci.* **1970**, *33*, 61.
- (52) Soni, V. K.; Stein, R. S. *Macromolecules* **1990**, *23*, 5257.

MA060060A